

Dual CNN based Channel Estimation for MIMO-OFDM Systems

Dwivedula Sahiti¹, Govind Srikanth¹, Adicherla Haneeth¹, A. Yuva Naga Teja¹,
C.Silpa¹

¹Department of Electronics and Communication Engineering, Malla Reddy Engineering College (A),
Secunderabad, Telangana, India

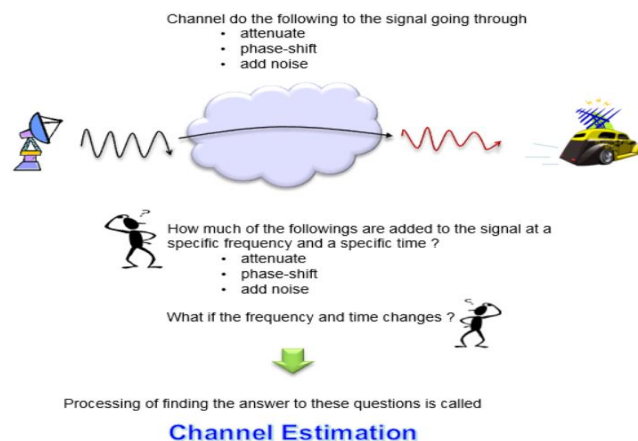
ABSTRACT

Recently, convolutional neural network (CNN)- based channel estimation (CE) for massive multiple-input multiple-output communication systems has achieved remarkable success. However, complexity even needs to be reduced, and robustness can even be improved. Meanwhile, existing methods do not accurately explain which channel features help the denoising of CNNs. In this , we first compare the strengths and weaknesses of CNN-based CE in different domains. When complexity is limited, the channel sparsity in the angle-delay domain improves denoising and robustness whereas large noise power and pilot contamination are handled well in the spatial frequency domain. Thus, we develop a novel network, called dual CNN, to exploit the advantages in the two domains. Furthermore, we introduce an extra neural network, called HyperNet, which learns to detect scenario changes from the same input as the dual CNN. HyperNet updates several parameters adaptively and combines the existing dual CNNs to improve robustness. Experimental results show improved estimation performance for the time-varying scenarios. To further exploit the correlation in the time domain, a recurrent neural network framework is developed, and training strategies are provided to ensure robustness to the changing of temporal correlation. This design improves channel estimation performance but its complexity is still low.

Index Terms—Deep learning, CNN, RNN, MIMO, channel estimation, robustness.

1.INTRODUCTION

All communication the signal goes through a medium (called channel) and the signal gets distorted or various noise is added to the signal while the signal goes through the channel. To properly decode the received signal without much errors are to remove the distortion and noise applied by the channel from the received signal. To do this, the first step is to figure out the characteristics of the channel that the signal has gone through. The technique/process to characterize the channel is called 'channel estimation'. This process would be illustrated as below.



Channel Estimation is the process of finding correlation between the array of complex numbers on the left and the array of complex numbers on the right.

Types of Channel Estimation Techniques Used in MIMO-OFDM

ORTHOGONAL FREQUENCY DIVISION MULTIPLEXING(OFDM)

In OFDM the large data stream to be transmitted is divided into parallel data streams. These data streams are fed to the orthogonal carriers at lower rate. Each subcarrier is modulated by using any one of the digital modulation schemes such as Binary Phase Shift Keying (BPSK), Quadrature Phase Shift Keying (QPSK) and Quadrature Amplitude Modulation (QAM). The data rate for each channel is low compared to the conventional data rate for a single-carrier modulation. However, the overall data rate is superior or comparable to the single-carrier modulation. Hence this scheme finds it's applications in most of the modern wireless broadcasting systems namely 802.11n (WIFI), WiMAX, LTE and Ultra-Wide Band (UWB) systems. In MIMO systems multiple antennas are used at both ends of the transmitter and receiver. Usage of MIMO-OFDM systems in modern wireless communication systems provides increased system capacity and coverage with robustness against multipath fading. Because of the unique properties of the MIMO and OFDM systems, these systems are used in high-speed wireless communication systems. MIMO can be subdivided into three main parts pre-coding, spatial multiplexing and diversity coding respectively. Precoding is one of the multi-stream beamforming techniques employed at the transmitter. In this method same type of signals are transmitted with weighted gains from each of the transmitting antennas in order to maximize the input signal power received at the receiver. It also reduces the multipath fading effect but, it requires CSI at the transmitter. Spatial multiplexing requires antenna configuration of the MIMO system. In this, a high data rate signal is split into a number of low data rate signals and each stream is transmitted using different antennas operating at the same frequency. At the receiver these signals arrive with different spatial signatures and it can easily separate these data stream into parallel channel.

3. PROPOSED METHOD

After introducing the multiuser MIMO-OFDM system and conventional CE methods, we present the existing AI-aided channel estimators, including DNN- and CNN-based CE in this section. Besides, we analyze the complexity of the current methods and introduce some techniques to improve robustness. We consider a BS with M antennas serving N_{ue} users, each with a single antenna. OFDM modulation with K subcarriers is used. The length of the transmit pilot sequence is P. The received signal at the Kth subcarrier of the BS is

$$Y_k = \sum_{n=1}^{N_{ue}} \sqrt{\rho_{n,k}} \mathbf{h}_{n,k} \otimes \mathbf{x}_{n,k}^* + Z,$$

where the channel between the BS and the nth user, $\mathbf{h}_{n,k} \in \mathbb{C}^{M \times 1}$, is constant over P time slots by virtue of block fading, $\mathbf{x}_{n,k} \in \mathbb{C}^{P \times 1}$ is the transmit pilot, $\rho_{n,k}$ is the transmit power, \otimes and $(\cdot)^*$ represent Kronecker product and Hermitian transpose and $Z \in \mathbb{C}^{M \times P}$ denotes the white Gaussian noise. To estimate the channel, the pilot sequence is orthogonal among different users from the same BS, yielding

$$\mathbf{x}_{n_1,k}^* \mathbf{x}_{n_2,k} = \begin{cases} P, & n_1 = n_2 \\ 0, & n_1 \neq n_2 \end{cases}.$$

Then, LS-CE can be expressed as

$$\hat{\mathbf{h}}_{n,k,LS} = \frac{1}{\sqrt{\rho_{n,k}P}} Y_k \mathbf{x}_{n,k},$$

In the subsequent discussion, we denote the true and the estimated channels of the nth user at all subcarriers as

$$\hat{\mathbf{H}}_{n,LS} \in \mathbb{C}^{M \times K}$$

However, the pilot sequences of the users from different BSs are not orthogonal, which leads to pilot contamination. LS estimation exploits no channel statistics. It has low complexity but poor performance. MMSE-CE improves performance by using the channel correlation in time, frequency, and antennas. Here, we assume that the channel is static within an OFDM block. For convenience, the $M \times K$ matrix is converted into an $MK \times 1$ channel vector by concatenating the columns, yielding

$$\hat{\mathbf{h}}_{n,LS} = \text{vec} \left(\hat{\mathbf{H}}_{n,LS} \right),$$

The linear MMSE (LMMSE) estimation of the channel vector is

$$\hat{\mathbf{h}}_{n,LMMSE} = \mathbf{R} \left(\mathbf{R} + \sigma^2 \mathbf{I}_{MK} \right)^{-1} \hat{\mathbf{h}}_{n,LS} = \mathbf{W}_{LMMSE} \hat{\mathbf{h}}_{n,LS},$$

The robust LMMSE estimation is expressed as

$$\begin{aligned} \hat{\mathbf{h}}_{n,m,RLMMSE} &= \mathbf{R}_f \left(\mathbf{R}_f + \sigma^2 \mathbf{I}_K \right)^{-1} \hat{\mathbf{h}}_{n,m,LS} \\ &= \mathbf{W}_{RLMMSE} \hat{\mathbf{h}}_{n,m,LS}. \end{aligned}$$

As a result, the complexity of the robust LMMSE estimation for each user is reduced to $O(MK \log K)$. In the following, it is denoted as RLMMSE. Compared with LMMSE, RLMMSE is less complicated but performs worse because RLMMSE does not exploit the spatial correlation and assumes that the power in the delay domain distributes uniformly

The estimated channel using the classic fully connected DNN can be written as

$$\hat{\mathbf{h}}_{n,DNN} = \mathbf{W}_L \cdots \beta \left(\mathbf{W}_2 \beta \left(\mathbf{W}_1 \hat{\mathbf{h}}_{n,LS} + \mathbf{b}_1 \right) + \mathbf{b}_2 \right) \cdots + \mathbf{b}_L,$$

where \mathbf{W}_i and \mathbf{b}_i denote the real multiplicative parameter matrix and the additive parameter vector for the i^{th} hidden layer, and $\beta(\cdot)$ is a nonlinear activation function. For fully connected DNN-based CE, the sizes of \mathbf{W}_i and \mathbf{b}_i increase with the numbers of antennas and subcarriers. The complexity of this architecture is larger than $O((MK)^2)$. The DL-based receiver reveals its superiority for extreme scenarios, such as insufficient pilots and nonlinear interference. However, complexity is the key restriction to many applications of DL in wireless communications. Thus, CNN-based receivers are used to simplify the architecture. In Fig. 1(b), the CE module is usually designed as a CNN-based denoiser, where the channels are regarded as two-dimensional pictures with frequency and antennas as height and width, the complexity is

$$O\left(\sum_{i=1}^L (cMKN_{i-1}N_i)\right)$$

where N_i denotes the number of filters in the i^{th} layer, the filter size is c . The input of the i^{th} layer is (M, K, N_{i-1}) , which means this input matrix has three dimensions with the sizes M, K, N_{i-1} , respectively. Transfer learning is a common method for adapting the trained network to a new environment. According , we can either reduce trainable parameters or exploit novel training strategies to save pilot resources online. Some architectures can adjust themselves without online transfer learning. The SNR feedback is utilized in while an extra DNN, called hyper-net, to adjust all the trainable

The channels are converted to a vector, and the correlation is fully utilized. (b) CNN-based CE. The channels are considered images, and the correlation of adjacent elements is more important. weights in. We take the DNN-based CE as an example to describe the architecture of hyper-net. For convenience, the process of a neural network is denoted as a function $f(a; b)$ in the following, where a is the input of the network and b contains all the trainable parameters of the network. Thus, Eq. (8) is rewritten as

$$\hat{\mathbf{h}}_{n,DNN} = f_{DNN}(\hat{\mathbf{h}}_{n,LS}; \mathbf{W}),$$

where \mathbf{W} denotes $[\mathbf{W}_1, \dots, \mathbf{W}_L; \mathbf{b}_1, \dots, \mathbf{b}_L]$, $f_{DNN}(\cdot; \cdot)$ is the process of the DNN-based CE. Then, a hyper-net is used to generate \mathbf{W} with some key parameters as an input. The process is expressed as

$$\mathbf{W} = f_{\text{hyper-net}}(l_{max}, \sigma^2, \dots; \mathbf{W}'),$$

where \mathbf{W}_0 denotes the trainable parameters in hyper-net.

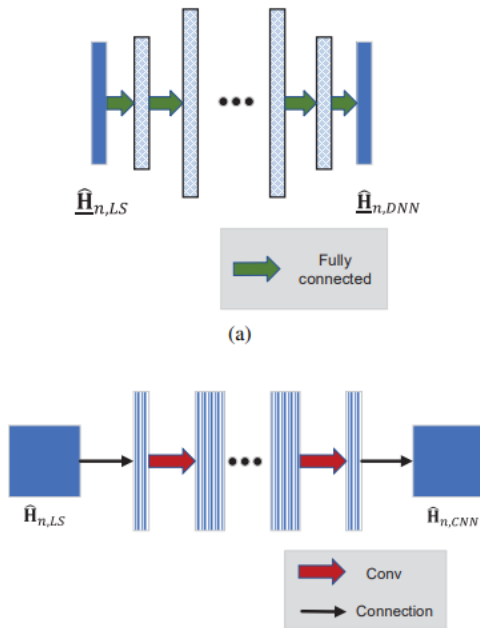


Fig. 1. (a) DNN-based CE

Thus, the entire process is

$$\hat{\mathbf{h}}_{n,DNN} = f_{DNN}(\hat{\mathbf{h}}_{n,LS}; f_{\text{hyper-net}}(l_{max}, \sigma^2, \dots; \mathbf{W}')).$$

After \mathbf{W}_0 is trained, the original trainable parameters, \mathbf{W} , are controlled by the key parameters, such as l_{max} and σ^2 . These key parameters are provided by the user, which is more convenient compared with retraining \mathbf{W} online.

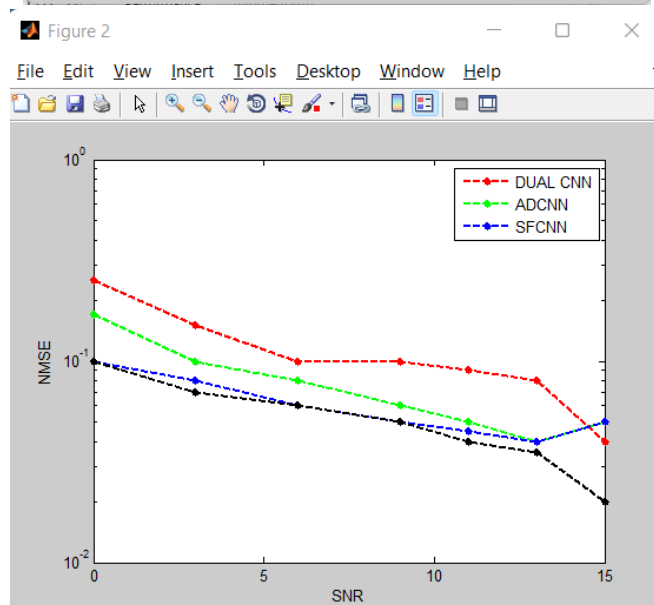
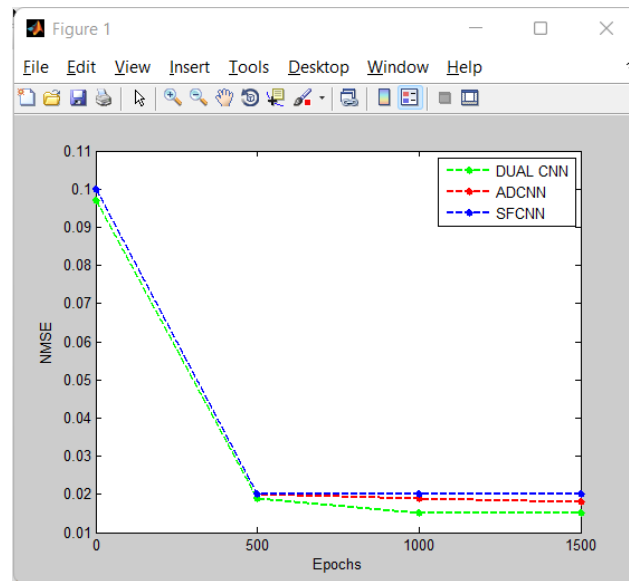
3. RESULTS

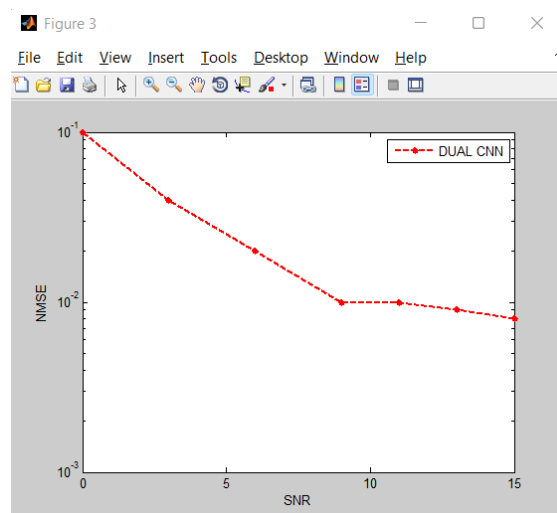
In the following, the low-complexity dual CNN is studied further. As shown in above result the dual CNN is compared with the SFCNN and the ADCNN. Although they have the same number of hidden layers and filters, the dual CNN converges faster because the dual CNN has a smaller network size in each domain. Meanwhile, the domain transform modules exploit the expert knowledge to help the dual CNN learn features quickly. The ADCNN converges as fast as thickened when training epochs < 200 but the ADCNN can reach better NMSE performance under the training SNR, i.e., 10 db.

To investigate the denoising performance of different methods, the power distribution in the AD domain is displayed using gray images, and the sparsity of the channel powering above result helps explain the noise power distribution after networks. In this simulation, SNR is set as 10 dB; thus, SFCNN is worse than ADCNN, whereas dual CNN is the best. The noise after SFCNN is still has power in the green circle, where the delay is larger than six. This result means that SFCNN has no global insight because the max delay is the most critical feature exploited by RLMMSE.

we train the three networks under SNR=5 db. Dual CNN still outperforms the other two methods and is better than LMMSE when SNR ≤ 7 dB. SFCNN is also nearly 3 dB better than RLMMSE when the

SNR is 0 dB. This result demonstrates that DL-based methods can outperform conventional methods under interference. ADCNN is better than SFCNN when SNR is low and the gap becomes smaller with the increase in SNR. This phenomenon means that ADCNN mistakenly takes the channel power as noise when trained under low SNR.





5. CONCLUSION

We first developed a CNN-based CE called dual CNN to take advantage of in the SF and AD domains. The channel's sparsity in the AD domain enables the CNN to handle most of the white noise, whereas the channel correlation in the SF domain helps ease interference. The SF domain's correlation also reduces the noise power so that the ADCNN has less possibility to be confused when distinguishing the channel and noise. Thus, the dual CNN has better performance and robustness than estimation in a single domain. We also introduced HyperNet, which does not require online training but performs better than the dual CNN and RLMMSE under the trained and untrained scenarios. We proposed an RNN framework to improve the CE performance by exploiting the temporal correlation of adjacent OFDM blocks. This framework is initiated with a trained dual CNN and learns to perform better than dual CNN. The robust design in this framework stabilizes its performance as long as the temporal correlation is larger than the assumption in the training set.

REFERENCES

- [1] E. G. Larsson, O. Edfors, F. Tufvesson, and T. L. Marzetta, "Massive MIMO for next generation wireless systems," *IEEE Commun. Mag.*, vol. 52, no. 2, pp. 186–195, Feb. 2014.
- [2] Y. Li, L. J. Cimini, and N. R. Sollenberger, "Robust channel estimation for OFDM systems with rapid dispersive fading channels," *IEEE Trans. Commun.*, vol. 46, no. 7, pp. 902–915, Jul. 1998.
- [3] O. Edfors, M. Sandel, J.-J. Van de Beek, S. K. Wilson, and P. O. Borjesson, "OFDM channel estimation by singular value decomposition," *IEEE Trans. Commun.*, vol. 46, no. 7, pp. 931–939, Jul. 1998.
- [4] T. J. O' Shea and J. Hoydis, "An introduction to deep learning for the physical layer," *IEEE Trans. Cogn. Commun. Netw.*, vol. 3, no. 4, pp. 563–575, Dec. 2017.
- [5] H. Ye, G. Y. Li, and B. H. Juang, "Power of deep learning for channel estimation and signal detection in OFDM systems," *IEEE Wireless Commun. Lett.*, vol. 7, no. 1, pp. 114–117, Feb. 2018.
- [6] Z.-J. Qin, H. Ye, G. Y. Li, and B.-H. Juang, "Deep learning in physical layer communications," *IEEE Wireless Commun.*, vol. 26, no. 2, Apr. 2019.
- [7] H. He, S. Jinn, C. Wen, F. Gao, G. Y. Li, and Z. Xu, "Model-driven deep learning for physical layer communications," *IEEE Wireless Commun.*, vol. 26, no. 5, pp. 77–83, Oct. 2019.
- [8] J. Kang, C. Chun, and I. Kim, "Deep-learning-based channel estimation for wireless energy transfer," *IEEE Commun. Lett.*, vol. 22, no. 11, pp. 2310–2313, Nov. 2018.
- [9] E. Balevi and J. G. Andrews, "One-bit OFDM receivers via deep learning," *IEEE Trans. Commun.*, vol. 67, no. 6, pp. 4326–4336, Jun. 2019.
- [10] S. Gao, P. Dong, Z. Pan, and G. Y. Li, "Deep learning-based channel estimation for massive MIMO with mixed-resolution ADCs," *IEEE Commun. Lett.*, vol. 23, no. 11, pp. 1989–1993, Nov.

2019.

[11] Q. Hu, F. Gao, H. Zhang, S. Jin, and G. Y. Li, "Deep learning for MIMO channel estimation: Interpretation, performance, and comparison," arXiv preprint arXiv:1911.01918, 2019.

[12] Y. Zhang, M. Alrabeiah, and A. Alkhateeb, "Deep learning for massive MIMO with 1-bit ADCs: When more antennas need fewer pilots," *IEEE Wireless Commun. Lett.*, vol. 9, no. 8, pp. 1273–1277, Aug. 2020.

[13] H. He, C. Wen, S. Jin, and G. Y. Li, "Deep learning-based channel estimation for beamspace mm Wave massive MIMO systems," *IEEE Wireless Commun. Lett.*, vol. 7, no. 5, pp. 852–855, Oct. 2018.

[14] M. Mehrabi, M. Mohammadkarimi, M. Ardakani, and Y. Jing, "Decision directed channel estimation based on deep neural network k -step predictor for MIMO communications in 5G," *IEEE J. Sel. Areas Commun.*, vol. 37, no. 11, pp. 2443–2456, Aug. 2019.

[15] C. Chun, J. Kang, and I. Kim, "Deep learning-based channel estimation for massive MIMO systems," *IEEE Wireless Commun. Lett.*, vol. 8, no. 4, pp. 1228–1231, Apr. 2019.